Advance Publication Cover Page



Temperature-dependent Oxidation of Carbon Nanotubes for Metal/semiconductor Separation

Sweejiang Yoo, Wenhui Yi,* Asif Khalid, Jinhai Si, and Xun Hou

Advance Publication on the web July 30, 2020 doi:10.1246/cl.200402

© 2020 The Chemical Society of Japan

Advance Publication is a service for online publication of manuscripts prior to releasing fully edited, printed versions. Entire manuscripts and a portion of the graphical abstract can be released on the web as soon as the submission is accepted. Note that the Chemical Society of Japan bears no responsibility for issues resulting from the use of information taken from unedited, Advance Publication manuscripts.

14

15

16

17

18

19

20

21

22

23

24

25

26

27

28

29

30

31

32

33

34

35

36

37

38

39

40

41

42

43

44

45

46

47

48

Temperature-dependent Oxidation of Carbon Nanotubes for Metal/semiconductor Separation

Sweejiang Yoo, ¹ Wenhui Yi, *1 Asif Khalid, ¹ Jinhai Si, ¹ and Xun Hou¹

¹Key Laboratory for Information Photonic Technology of ShaanXi Province & Key Laboratory for Physical Electronics and Devices of the Ministry of Education, School of Information and Electronics Engineering, Xi'an Jiaotong University, 710049, China

E-mail: yiwenhui@mail.xjtu.edu.cn

49

50

51

52 53

55

56

57

58

60

61

62

63

64

65

66

67

68

69

70

73

74

75

76

80

81

82

83

84

85

86

87

88

89

90

91

92

93

94

95

The speculated temperature has induced/reversed the oxidation of SDS-dispersed SWCNTs in water, in which the oxidation triggers the reorganization of SDS structure on SWCNTs to afford selective adsorption in gel chromatography. Molecular dynamics simulations are performed to elucidate how the oxidation affects the assembly of SDS structure on a SWCNT. We found the formation of high-density SDS coatings over oxidized SWCNT than unoxidized SWCNT, which implies the temperature-dependent oxidation enables the metal/semiconductor (M/S) separation of SWCNTs.

2 Keywords: SWCNTs, Temperature, M/S Separation

Carbon nanotubes have remarkable electrical, optical and mechanical properties that make them promising in many applications, such as energy harvest and storage, photoswitches, and molecular electronics. ¹⁻⁶ However, assynthesized single-walled carbon nanotubes (SWCNTs) are complex mixture consisting of different electronic type and species (n,m). Noteworthy, the peculiar properties of SWCNTs are relying on the specific subpopulations present. Hence, the separation of SWCNTs to identical subpopulations is critical for their basic research and technical applications.

Several methods have ability of separating SWCNTs by electronic type, including DNA- wrapping, density gradient ultracentrifugation (DGU), gel electrophoresis, polymer extraction, and aqueous two-phase extraction.⁷⁻¹⁵ chromatography-based separation approach was devised in 2009, where the polysaccharide gel was used as a separation medium.¹⁶⁻¹⁸ Like ion-exchange chromatography, the polysaccharide gel is used in biochemical separation widely. Tanaka et al. and Moshammer et al. observed an intriguing phenomenon when exposing the sodium dodecyl sulfate (SDS) -dispersed SWCNTs to the gel matrix. 18, 19 The semiconducting species (sc-SWCNTs) are trapped or strongly attracted to the polysaccharide gel primarily, whereas metallic species (m-SWCNTs) passed through the gel. This straightforward chromatographic method is quick, scalable, and outputting gel-free SWCNTs. 18, 19

The selective retention of sc-SWCNTs has enables the M/S separation, where it is proposed that difference SDS coverage and structures are formed for m-SWCNTs and sc-SWCNTs. $^{20\text{-}22}$ In 2012, Hirano et al. revealed the net absorbability (αK) of SWCNTs onto the gel matrix, which has a proportional linear relationship with temperature, indicating the significant contribution of temperature factor in scaling interaction strength between SDS-SWCNTs and gel matrix. 23 Several publications incorporated temperature

effect onto gel chromatography in enhancing the different in interactions of various (n, m) SWCNTs with the gel matrix. As to separate single species or improving the M/S separation at large diameter regime. ²⁴⁻²⁸ This method has advantages of simplicity, low cost, and high efficiency. While the use of temperature has been effective in separation of SWCNTs thus underlying mechanism is little understood.

In this context, we attempt to discuss how the temperature affects the assembly of SDS on SWCNT. The SWCNTs are known to easily oxidized in an acidic medium and even neutral solution. According to Nish et al., the oxidation of SDS-dispersed SWCNTs in water can be reversed by heating.²⁹ At the same time, several recent publications have utilized the redox effect to improve the metal/semiconductor separation.³⁰⁻³² We, therefore, speculate temperature could reduce/oxidize the SWCNTs, that yields selective adsorption of sc-SWCNTs or m-SWCNTs at different temperature. Herein, we presented an experimental study of the selective adsorption of SWCNTs at different temperatures. The temperature can affect the oxidation level of a SWCNT. Molecular dynamics simulations are performed to show the oxidation level could induce the reorganization of SDS arrangement, hence explaining the enrichment-temperature relationship observed. The experiment method for selective adsorption (M/S separation) is adapted from literature with minor modifications. ²⁴ Specifically, the temperature range is extended to 50°C for the selective adsorption of m-SWCNTs. The HiPCo SWCNTs were purchased from NanoIntegris (Canada), with a length of 0.1 to 1.0 µm and a diameter 0.8 to 1.2 nm. The cross-linked allyl dextran gel filtration media (Sephacryl® S200HR, G.E. Healthcare), sodium dodecyl sulfate (SDS, Sigma Aldrich ≥99%) and sodium deoxycholate (DOC, Alfa Aesar ≥98%) were used as purchased without further purification. A 100 mg of HiPco SWCNTs powder was suspended in 100 ml aqueous 0.5 wt.% SDS by tip sonication (Scientz -IID, 120W) for 2h while being immersed in a water bath (12°C). The dispersion was centrifuged at 215000g (Sorvall WX100) for 0.5h to sediment out amorphous carbon and large bundles. 80-90% of supernatant was extracted using pipettes and used for the separation process.

Two 5 ml columns were filled with Sephacryl S200HR as a filtration medium. The parent suspension, 0.5 wt.% SDS solution and the gel column were immersed in a water bath (Scientz DC-3010). To perform the M/S separation at room temperature, the water bath was pre-equilibrated at 25°C (room temperature) for 20 min. The column was then

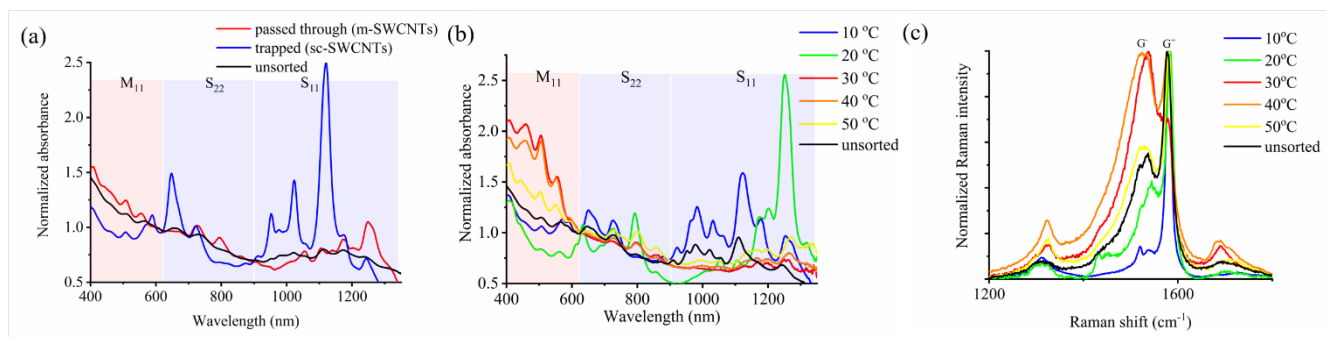


Figure 1 Absorption spectra of SWCNTs that underwent M/S separation (a) passed through SWCNTs and trapped SWCNTs at room temperature (b) trapped SWCNTs at various temperatures (trapped). All the spectra were normalized to 627 nm for ease of comparison and clarity. (c) The Raman spectra of trapped SWCNTs at different temperatures. All the spectra were normalized to G band for ease of comparison and clarity

flushed with an SDS solution using a peristaltic pump (Longer BT100, ~10 rpm) before applying the parent suspension. The pass-through fraction was collected. Subsequently, the columns were flushed with SDS solution to elute the unbound SWCNTs. The trapped fraction was obtained by applying 2 wt.% DOC solution to the columns.

Next, the M/S separation was conducted at five different temperatures, which include 10°C, 20°C, 30°C, 40°C, and 50°C. The parent suspension was initially loaded onto the columns at 10°C, in which the pass-through fraction was collected and used for the next separation trial (at each temperature, the separation was performed by loading the pass-through fraction from the previous stage). The trapped fraction was collected.

Optical absorbance spectra were measured using an ultraviolet—near-infrared spectrophotometer (LAMDA 950, Perkin Elmer). Raman spectra for 532 nm excitation were measured using a confocal Raman microscope (HR800, Horiba).

The molecular dynamics (MD) simulation is adapted from literature with minor modifications.³³ The MD simulations were performed using the Forcite module from Material Studio, which the COMPASS II force field (Condensed-phased Optimized Molecular Potential for Atomistic Simulation Studies II) modeled the atomic interaction.34 COMPASS is an all-atom force field for atomistic simulation of common organic molecules, which provides a valid description for SWCNT composites. The simulations were conducted with the NVT ensemble at a temperature of 298K in a rectangular box with dimensions of approximately 74 Å (x-axis) and 74 Å (y- and z-axis). The electrostatics were treated by using the Ewald summation method with an accuracy of 0.001 kcal/mol, whereas the van der Waals interactions were treated by using the atom-based summation method with 12.5 Å cutoff distance. The temperature was controlled by using a Nose-Hoover-Langevin thermostat. The integration time step was set to 1

The microscopic information of an uncharged or charged SWCNT with surfactants was investigated. A (6,6) SWCNT (with a diameter of 0.81 nm and a length of 74 Å) was selected as a representative SWCNT. The SWCNT was kept rigid in a water box (74Å x 74Å x 74Å) throughout the simulations. The system contained a SWCNT, 48 dodecyl

sulfate ions, and approximately 2700 water molecules. Initially, the surfactants were scattering placed inside the box. In the uncharged SWCNT system, 48 sodium ions were added, whereas, in the charged SWCNT, 47 sodium ions were added. The 5ns calculations were performed for each system, that is, uncharged or charged SWCNT/SDS system. We assigned one positive charge per 100 carbon atoms to study a charged SWCNT system according to literature, which also comparable to the experimental data.^{33, 35} The charge was distributed to each carbon atom of the SWCNT evenly. The total charge of the SWCNT was set to +7 for the charged SWCNTs systems.

Initially, the M/S separation experiment is performed at room temperature. The optical absorption spectra (Figure 1(a)) show the SWCNTs underwent M/S enrichment when SDS -dispersed SWCNTs were loaded into the gel matrix at room temperature. The S_{22} represents the E_{22} optical transition of sc-SWCNTs, while M_{11} represents the E_{11} optical transition of m-SWCNTs. The sc-SWCNT were trapped to the gel primarily, whereas m-SWCNTs passed through the gel matrix. The semiconducting enrichment is evidenced by the intensified of S_{22} peaks and attenuation of M_{11} peaks, whereas attenuation of S_{22} peaks evidencing the metallic enrichment. By performing optical absorption spectroscopy evaluation, the purities of sc-SWCNTs and m-SWCNTs are estimated to be about 83% and 25%, respectively. 36

In subsequent, the M/S separation experiment was conducted at five different temperatures. Based on the optical spectra of trapped SWCNTs at different temperatures (Figure 1(b)), sc-SWCNTs were separated at 10°C and 20°C, as evidenced by the sharp S₂₂ and S₁₁ peaks, as well as strong suppression of M₁₁ peaks. While the separation temperature increased from 30°C to 40°C, m-SWCNTs are selectively enriched according to the sharp M₁₁ peaks and diminished S₂₂ peaks. Based on these curves, the purities of sc-SWCNTs are estimated to be about 77% (10°C) and 92% (20°C), while purities of m-SWCNTs are about 85% (30°C) and 80% (40°C). Although the obtained purities are below par in comparison to recent publications, it revealed the temperature effect enhanced the M/S separation in gel chromatography.

We further compare the Raman spectra of trapped SWCNTs at different temperatures (Figure 1(c)). Due to the quantum confinement effect, the tangential G mode in

Q

SWCNTs (between 1500–1600 cm⁻¹) splits into G⁻ and G⁺ submodes, which G⁺ for atomic displacements along the tube axis and G⁻ for modes with atomic displacement along the circumferential direction.³⁷ The broadening of G⁻ is typically assigned to the presence of m-SWCNTs because of the availability of a large number of free electrons in m-SWCNTs. In Figure 1(c), the G⁻ is attenuated, which suggests the separation of sc-SWCNTs from m-SWCNTs. The broadening of G⁻ becomes prominent as the temperature increased, implying the enrichment of m-SWCNTs. The Raman spectra are consistent with the optical absorption analysis.

The van der Waals, steric and electrostatic interactions are responsible for the adsorption of nanotubes onto gel matrix. Hence, any difference in the surfactant structure will therefore exert influence on these interactions. It generally accepted that the SDS molecules are lying flat around the sc-SWCNTs.³⁸ In contrast, SDS molecules form ordered cylindrical micelles around m-SWCNTs, in which nanotube behaves like the core with the SDS extended radially from the center. Niyogi et al. further evidenced a higher packing density of SDS on m-SWCNTs than sc-SWCNTs. ³⁹ These are implying the formation of different SDS structure around m-/sc-SWCNT to enable the M/S separation.

Boualem Hammouda found that micelle aggregation number of SDS decreases with increasing temperature via small-angle neutron scattering (SANS) technique.⁴⁰ Liu et al. have speculated that lowering temperature reduces the solubility of the SDS surfactant, inducing additional SDS molecules to aggregate on the nanotube surfaces, forming high-density SDS coatings.²⁴

Analogously, in our case, smaller SDS micelle structures formed around the sc-SWCNTs at lower temperatures (10-20°C), making them physisorbed on the gel surface. The mSWCNTs are less susceptible to being physisorbed onto the gel surface because the high packing density and ordered cylindrical micelles have overcome the van der Waals interaction.²⁵ This may explain why most m-SWCNTs are flow-through the gel matrix at low temperature. Inversely, the SDS micelles shrank in size and got loosely packed as temperature increased, promoting the physisorption of SWCNTs onto the gel matrix.

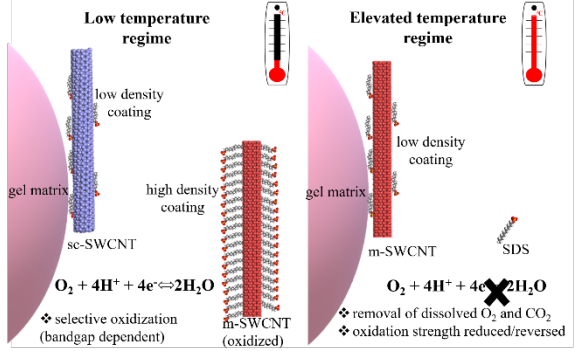


Figure 2 The graphical illustration of how the temperature affects (induces/reverses) the oxidation of SWCNTs that enables the M/S separation.

It is generally accepted that temperature affects the oxidation level of SWCNTs, in which the oxidation is

reversible at elevated temperature due to O², H⁺/H₂O couple oxidizing strength is reported to vary with temperature.²⁹ Importantly, oxidation leads to change in composition and/or spatial arrangement of the surfactant around the SWCNTs due to the presence of positive charges from oxidized SWCNTs.^{25, 32, 33, 35, 41}. Besides, the reduction potential of SWCNT is reported to increase with increasing bandgap or bandgap-dependent, implying m-SWCNTs with vanishingly bandgap are prone to oxidation than sc-SWCNTs.^{29, 35, 42}

From literature, the selective oxidation through HCl and CO₂-bubbling successfully reduce the adsorbability of the m-SWCNTs onto the gel matrix.^{30, 31} In contrast, Yang et al. have proposed that the prevention of the oxidation of SWCNTs through the addition of NaOH, that neutralizing the H⁺ ions in aqueous solution.⁴¹ Importantly, Nish et al. revealed the oxidation of SDS-dispersed SWCNTs in water could be reversed by heating.²⁹ We, therefore, reasoning the temperature has induces/reverses the oxidation of SWCNTs that enhances the M/S separation (Figure 2).

At lower temperatures (10-20°C), the O₂ combines with H⁺ in the water, which removed an electron from SWCNT and subsequently triggered the reorganization of the SDS layer.²⁹ We postulated the m-SWCNTs, were they covered with more SDS molecules in comparison to sc-SWCNTs, as they are more susceptible to the oxidation in the presence of H⁺ and O₂ because of smaller reduction potential. The highdensity SDS coating on m-SWCNTs is making them less likely to be physisorbed on the gel surface than sc-SWCNTs, that allows the metal/semiconductor separation. However, the dissolved gases in aqueous solution (e.g., O₂ and CO₂) decrease at elevated temperature, which diminishing the oxidizing strength of O₂, H⁺/H₂O couple.²⁹ It then again triggered the reorganization of the SDS layer on m-SWCNTs, making them covered with fewer SDS molecules and eventually physisorbed on the gel surface.

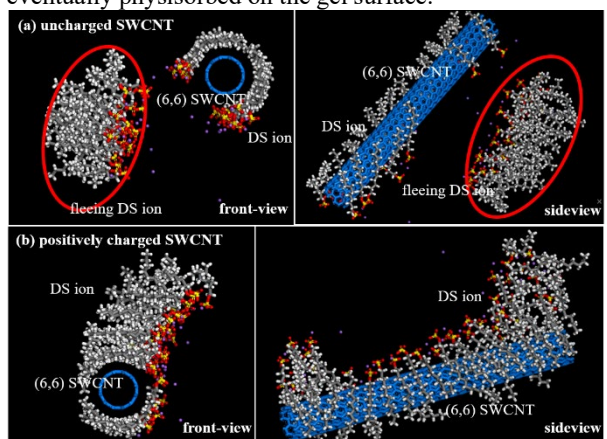


Figure 3 The assembly of SDS surfactants around (a) an uncharged SWCNT (b) positively charged SWCNT at 5ns. The water molecules are hidden for clarity.

Table 1. The number of SDS in the vicinity of the uncharged and positively charged SWCNT. They are estimated according to the number of S atoms of DS existing at the distance of 8-20Å from the SWCNT's axial center.

	Uncharged SWCNT	Positively charged SWCNT
Number of surfactant ions	21	30
Average ion surface coverage (ion/nm²)	1.11	1.59

36

37

38

39

40

41

42

43

44

45

46

47

48

49

50

51

52

53

54

55

56

57

58

59

60

61

62

63

64

65

66

67

68

69

70

71

72

73

74

75

76

77

78

79

80

81

82

83

85

86

87

88

90

91

92

To evaluate the oxidation triggers the reorganization of SDS, we then simulated the assembly of SDS on oxidized/unoxidized SWCNT. The positively charged SWCNT exemplifies the oxidization of SWCNT under low temperature, whereas uncharged SWCNT represents the suppression of oxidization under elevated temperature. For the uncharged system, the SDS migrated towards the SWCNT surface. In the equilibrium state at 5ns (Figure 3(a)), the SDS wrapped around the SWCNT and formed a cylindrical micelle structure on the nanotube's surface, where the SDS aligned in perpendicular to the nanotube axial.⁴³ The SDS surfactant constitutes a hydrophilic head group and a hydrophobic tail. The hydrophilic head was leaned toward the water molecules, whereas the hydrophobic tail was attracted to the SWCNT surface due to van der Waals attraction. This behavior may create a distribution of negative charges that prevent their aggregation and induced stable suspensions in water.

From Figure 3(b), the positively charge SWCNT has a higher density of SDS surfactants in comparison to the uncharged SWCNT ((1.59 ion/nm² vs. 1.11 ion/nm²). There were 30 SDS surfactants in the vicinity of the positively charged SWCNT, but only 21 SDS surfactants were assembled around the uncharged SWCNT, as summarized in Table 1. The oxidation is favoring the formation of a compact cylindrical micelle structure on the nanotube's surface.

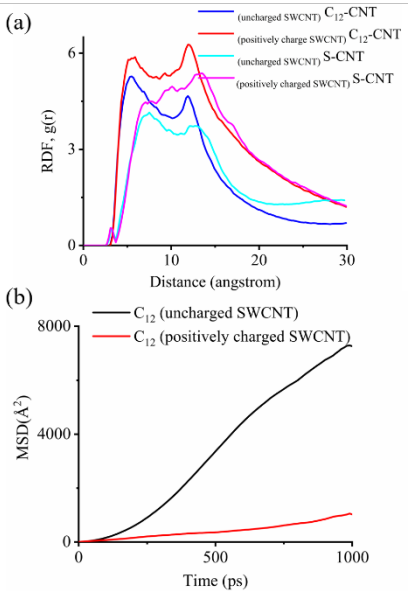


Figure 4 (a) RDF of CNTs to C_{12} (tail of SDS) and S (head of SDS) in SWCNT/water/surfactant systems, for charged and uncharged SWCNT. (b) MSD of C_{12} (tail of SDS) in SWCNT/water/surfactant systems in the period 4-5ns.

The mean-squared displacement (MSD) and radial distribution function (RDF) are used to describe the structural transformation of molecules in SWCNT/water/SDS during

the equilibration. RDF is the probability of finding an atom at a distance (r) from the given reference atom. 44 From Figure 4 (a), the first peaks for carbon atoms of the surfactant tail end (C₁₂ for SDS) and sulfur atom of the head (S for SDS) are observed at approximately 5 Å and 7 Å, respectively. At the short distances (less than atomic diameter), RDF is zero due to the strong repulsive forces, and within SWCNTs, there are no surfactant molecules. The RDF of positively charged SWCNT has more substantial value for CNT-C₁₂ and CNT-S than uncharged SWCNT, indicate a higher amount of SDS assembled around the SWCNT, which consistent with the observation (Table 1). For the positively charged SWCNTs, the profiles of C₁₂ and S are found to have a prominent secondary peak at 12 Å and 10-17 Å, respectively, which imply the presence of double layers on the SWCNT surface or higher packing of SDS. The prominent first and the second peak with increasing distance indicate a more efficient packing of surfactant molecules around SWCNT even at a larger distance. The RDF then fell and passed through a minimum value, implying unfavorable locations of having an association between surfactant molecules and CNTs.

MSD is determines based on the position of the particle over time. We analyzed the MSD of C₁₂ (tail of SDS) for positively charged SWCNT and uncharged SWCNTs in SWCNT/water/surfactant systems at the period 4-5ns, which we considered the system had reached equilibrium (Figure 4(b)). The low displacement of C₁₂ for positively charged SWCNT implies most SDS were assembled and entangled around the rigid SWCNT. In sharp contrast, the high displacement of C₁₂ for uncharged SWCNT revealed large numbers of SDS were fleeing and having free movement in the water. It should be noted that the displacement of molecules is related to particle mobility and a significant displacement increment reveals a more energetic activity. It is logical to correlate the weak activity infers the higher numbers of SDS molecules being assembled around the SWCNT. The strong electrostatic attraction and van der Waals have restricted the fleeing and free movement of SDS in water, thus explains the low MSD value.

In summary, we demonstrate the temperature effect enhanced the M/S separation of SWCNTs in gel chromatography. It is proposed, which in agreement with the literature, the temperature has induced/reversed the oxidation of SDS-dispersed SWCNTs in water, in which the oxidation triggers the reorganization of the SDS structure on SWCNTs to afford selective adsorption.²⁹ MD simulations are carried out to illustrate the temperature-dependent oxidation exerts influence over the assembly of SDS on a SWCNT. The positively charge SWCNT, as a model for oxidized SWCNT under low temperature, has a high-density SDS coating (1.59) ion/nm² vs. 1.11 ion/nm²) in comparison to the uncharged SWCNT (model for unoxidized SWCNT under elevated temperature). The RDF and MSD analysis supported the formation of high-density SDS coating on oxidized SWCNT, implying the temperature-dependent oxidation enhances the metal/semiconductor separation of SWCNTs.

We thank Miss Wang and Miss Lu at the Instrument Analysis Center of Xi'an Jiaotong University for their assistance with

33

2

3

5

6

9

10

11

12

13

14

15

16

17

18

19

20

21

22

23

24

25

- Raman and optical absorbance spectra measurement. (This
- research was generously supported by the Natural Science 2
- Foundation of China (No. 61275179, and 60970815), the 3
- 4 Natural Science Basic Research Plan in Shaanxi Province of
- China (Program No. 2016JM8047), the Fundamental Funds
- for the Central Universities (No. xjj2015112), and ShaanXi
- Province Administration of Traditional Chinese Medicine
- (15-ZY036).)

References and Notes

- 10 1 R. E. Smalley, Carbon nanotubes: synthesis, structure, properties, 11 and applications. Editor, Springer Science & Business Media, 2003, 12
- 13 2 S. Li, Y. Feng, et al., Carbon 2016, 109, 131-140.
- 14 Y. Feng, X. Zhang, et al., Carbon 2010, 48, 3091-3096.
 - Y. Feng, W. Feng, et al., Carbon 2007, 45, 2445-2448.
- 5 W. Feng, W. Yi, et al., Journal of applied physics 2005, 98, 034301.
- Y. Feng, W. Feng, et al., Journal of Applied Physics 2007, 102, 053102.
- 19 7 X. Tu, S. Manohar, et al., Nature 2009, 460, 250-253.
- G. Ao, J. K. Streit, et al., Journal of the American Chemical Society **2016**, 138, 16677-16685.
 - M. Zheng, A. Jagota, et al., Science 2003, 302, 1545-1548.
- 10 M. S. Arnold, A. A. Green, et al., Nature Nanotechnology 2006, 1,
- 11 M. S. Arnold, S. I. Stupp, et al., Nano Letters 2005, 5, 713-718.
- 20 21 22 23 24 25 26 27 28 29 30 12 C. Y. Khripin, J. A. Fagan, et al., Journal of the American Chemical Society 2013, 135, 6822-6825.
- 13 N. K. Subbaiyan, S. Cambré, et al., Acs Nano 2014, 8, 1619-1628.
 - 14 A. Nish, J.-Y. Hwang, et al., Nature nanotechnology 2007, 2, 640.
- 15 T. Tanaka, H. Jin, et al., Applied Physics Express 2008, 1, 114001-114006.
- 31 32 33 34 35 16 T. Tanaka, H. Jin, et al., Physica Status Solidi (b) 2009, 246, 2490-
 - 17 T. Tanaka, H. Jin, et al., Nano Letters 2009, 9, 1497-1500.
- 18 T. Tanaka, Y. Urabe, et al., Applied Physics Express 2009, 2, 125002-36 37
- 19 M. Kai, F. Hennrich, et al., Nano Research 2009, 2, 599-606.
- 38 39 20 C. A. Silverabatista, D. C. Scott, et al., Journal of Physical Chemistry C 2011, 115, 9361-9369.
 - 21 K. Tvrdy, R. M. Jain, et al., Acs Nano 2013, 7, 1779-1789.
- 41 22 R. M. Jain, K. Tvrdy, et al., ACS Nano 2014, 8, 3367-3379.
- 23 A. Hirano, T. Tanaka, et al., Acs Nano 2012, 6, 10195-10205.
- 24 H. Liu, T. Tanaka, et al., Nano Letters 2013, 13, 1996-2003.
- 25 I. Yahya, F. Bonaccorso, et al., Carbon 2015, 93, 574-594.
- 45 26 B. Thendie, H. Omachi, et al., Japanese Journal of Applied Physics 46 **2017**, 56, 065102-065110.
- 47 27 S. Yoo, W. Yi, et al., physica status solidi (b) n/a, 1900714 48 10.1002/pssb.201900714.
- 49 28 G. Wang, X. Wei, et al., Carbon 2018, 129, 745-749.
- 29 A. Nish, R. J. Nicholas, Physical Chemistry Chemical Physics 2006, 8, 3547-3551.
- 30 J. Cui, W. Su, et al., ACS Applied Nano Materials 2018, 2, 343-350.
- 31 Y. Ichinose, J. Eda, et al., The Journal of Physical Chemistry C 2017, 121, 13391-13395.
- 32 H. Gui, J. K. Streit, et al., Nano Letters 2015, 15, 1642-1646.
- 33 A. Hirano, T. Kameda, et al., ChemNanoMat 2016, 2, 911-920.
- 34 H. Sun, Z. Jin, et al., Journal of Molecular Modeling 2016, 22, 47-56.
- 58 59 35 M. Zheng, B. A. Diner, Journal of the American Chemical Society 2004, 126, 15490-15494.
- 60 36L. Huang, H. Zhang, et al., The Journal of Physical Chemistry C 2010, 114, 12095-12098.
- 62 37 P. Singh, S. Campidelli, et al., Chemical Society Reviews 2009, 38, 63 2214-2230.
- 38 J. G. Clar, C. A. Silvera Batista, et al., Journal of the American 65 Chemical Society 2013, 135, 17758-17767.
- 39 S. Niyogi, C. G. Densmore, et al., Journal of the American Chemical Society 2009, 131, 1144-1153.

- 40 B. Hammouda, Journal of Research of the National Institute of 69 Standards and Technology 2013, 118, 151-167.
- 70 41 D. Yang, J. Hu, et al., Advanced Functional Materials 2017, 27, 71 72 1700278-1700287.
- 42 M. S. Strano, C. B. Huffman, et al., The Journal of Physical 73 74 75 Chemistry B 2003, 107, 6979-6985.

76 77

- 43 W. H. Duan, Q. Wang, et al., Chemical Science 2011, 2, 1407-1413.
- 44 F. Razmimanesh, S. Amjad-Iranagh, et al., Journal of Molecular Modeling 2015, 21, 165-178.